J|A|C|S ARTICLES

Published on Web 09/11/2009

Proton-Driven Amide Bond-Cleavage Pathways of Gas-Phase Peptide Ions Lacking Mobile Protons

Benjamin J. Bythell,[†] Sándor Suhai,[†] Árpád Somogyi,[‡] and Béla Paizs*,[†]

Department of Molecular Biophysics, Im Neuenheimer Feld 580, German Cancer Research Center, 69120 Heidelberg, Germany, and Department of Chemistry, University of Arizona, Tucson, Arizona 85721

Received May 27, 2009; E-mail: B.Paizs@dkfz.de

Abstract: The mobile proton model (Dongré, A. R.; Jones, J. L.; Somogyi, A.; Wysocki, V. H. *J. Am. Chem. Soc.* **1996**, *118*, 8365−8374) of peptide fragmentation states that the ionizing protons play a critical role in the gas-phase fragmentation of protonated peptides upon collision-induced dissociation (CID). The model distinguishes two classes of peptide ions, those with or without easily mobilizable protons. For the former class mild excitation leads to proton transfer reactions which populate amide nitrogen protonation sites. This enables facile amide bond cleavage and thus the formation of *b* and *y* sequence ions. In contrast, the latter class of peptide ions contains strongly basic functionalities which sequester the ionizing protons, thereby often hindering formation of sequence ions. Here we describe the proton-driven amide bond cleavages necessary to produce *b* and *y* ions from peptide ions lacking easily mobilizable protons. We show that this important class of peptide ions fragments by different means from those with easily mobilizable protons. We present three new amide bond cleavage mechanisms which involve salt-bridge, anhydride, and imine enol intermediates, respectively. All three new mechanisms are less energetically demanding than the classical oxazolone b_n-y_m pathway. These mechanisms offer an explanation for the formation of *b* and *y* ions from peptide ions with sequestered ionizing protons which are routinely fragmented in large-scale proteomics experiments.

1. Introduction

Protein identification in the rapidly growing field of proteomics[1] is primarily based on the analysis of proteolytic peptides using tandem mass spectrometry (MS/MS). Most commonly proteins are digested with trypsin which cleaves selectively after arginine (R) and lysine (K) residues (except when these are followed by proline). Thus, most tryptic peptides contain a single R or K at their C-terminus. These peptides are usually ionized by protonation and introduced into the mass spectrometer by means of electrospray ionization (ESI)[2a] or matrix-assisted laser desorption/ionization (MALDI).[2b] ESI of average-sized tryptic peptides predominantly leads to multiply charged peptide ions, while MALDI forms singly protonated peptides. In the most widely used instruments these protonated peptides are excited by collisions with inert gas atoms/molecules to induce dissociation (collision-induced dissociation (CID)). The abundances and mass-to-charge ratios (*m*/*z*) of the resulting charged fragments are then measured as a product ion spectrum. Under low-energy CID conditions protonated peptides are often dissociated by cleavage of amide bonds to produce b_n and y_m ion series.[3] The information contained in the *m*/*z* differences between neighboring b_n and y_m ions is then used to determine the primary structure of peptides; currently this task is almost exclusively carried out with the use of sequencing software.[1] For this strategy to be effective, the fragmentation models[4] utilized in these software packages need to reflect the chemistry taking place in the mass spectrometer.

The critical role played by the ionizing proton(s) in the cleavage of backbone amide bonds has been studied using a wide variety of experimental and theoretical strategies.[5−7] ESI and MALDI are soft ionization techniques which produce peptide ion populations with low average internal energies. This means that the vast majority of these ions are generated with ionizing protons occupying the energetically most favored (generally the most basic) protonation sites such as the arginine,

[†] German Cancer Research Center.
[‡] University of Arizona.

(1) (a) Aebersold, R.; Goodlett, D. R. *Chem. Rev.* **2001**, *101*, 269–296. (b) Steen, H.; Mann, M. *Nat. Rev. Mol. Cell. Biol.* **2004**, *5*, 699–711.
(2) (a) Yamashita, M.; Fenn, J. B. *J. Phys. Chem.* **1984**, *88*, 4451–4459. (b) Karas, M.; Hillenkamp, F. *Anal. Chem.* **1988**, *60*, 2299–2301.
(3) (a) Roepstorff, P.; Fohlmann, J. J. *Biomed. Mass Spectrom.* **1984**, *11*, 601. (b) Biemann, K. *Biomed. Environ. Mass Spectrom.* **1988**, *16*, 99.
(4) Paizs, B.; Suhai, S. *Mass Spectrom. Rev.* **2005**, *24*, 508–548.
(5) (a) Biemann, K.; Martin, S. A. *Mass Spectrom. Rev.* **1987**, *6*, 1. (b) Burlet, O.; Yang, C. Y.; Gaskell, S. J. *J. Am. Soc. Mass Spectrom.* **1992**, *3*, 337. (c) Tang, X.; Boyd, R. K. *Rapid Commun. Mass Spectrom.* **1992**, *6*, 651. (d) Tang, X.-J.; Thibault, P.; Boyd, R. K. *Anal. Chem.* **1993**, *65*, 2824. (e) Johnson, R. S.; Krylov, D.; Walsh, K. A. *J. Mass Spectrom.* **1995**, *30*, 386. (f) Burlet, O.; Orkiszewski, R. S.; Ballard, K. D.; Gaskell, S. J. *Rapid Commun. Mass Spectrom.* **1992**, *6*, 658.
(6) (a) Dongré, A. R.; Jones, J. L.; Somogyi, A.; Wysocki, V. H. *J. Am. Chem. Soc.* **1996**, *118*, 8365–8374. (b) McCormack, A. L.; Somogyi, A.; Dongre, A. R.; Wysocki, V. H. *Anal. Chem.* **1993**, *65* (20), 2859. (c) Somogyi, A.; Wysocki, V. H.; Mayer, I. *J. Am. Soc. Mass Spectrom.* **1994**, *5* (8), 704. (d) Wysocki, V. H.; Tsaprailis, G.; Smith, L. L.; Breci, L. A. *J. Mass Spectrom.* **2000**, *35* (12), 1399. (e) Tsaprailis, G.; Nair, H.; Somogyi, A.; Wysocki, V. H.; Zhong, W.; Futrell, J. H.; Summerfield, S. G.; Gaskell, S. J. *J. Am. Chem. Soc.* **1999**, *121* (22), 5142.

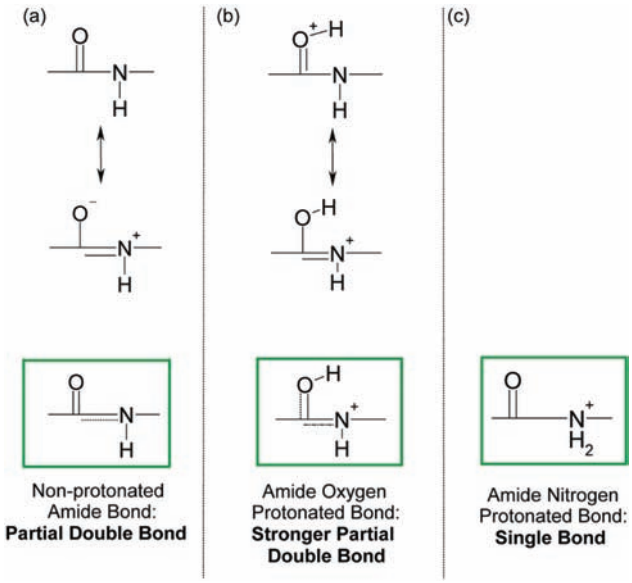

Figure 1. Effect of amide bond protonation. Resonance structures and representative superposition structures (in the green boxes) of the three protonation types. (a) Protonation at the N-terminus or a basic residue; (b) amide oxygen protonation; (c) amide nitrogen protonation.

lysine, and histidine side chains and the N-terminal amino group. In these structures the peptide groups remain neutral and their partial double bond character hinders formation of b_n and y_m ions (Figure 1a). In order to rationalize the formation of these sequence ions numerous authors have suggested[5,6] that transfer of an ionizing proton to a peptide bond is the first step of the dissociation chemistry, i.e. that amide bonds are actually cleaved on charge-directed (proton-driven) fragmentation pathways. Initial proton mobilization away from the most basic protonation sites is usually achieved via transfer to amide oxygen sites. These sites are still reasonably energetically favorable, but populating them comes with the adverse effect of strengthening the amide bond[6] (Figure 1b). Additional energy is required to mobilize an ionizing proton to an amide nitrogen site;[6] however, this proton transfer has the desired effect of weakening the amide bond (reducing the bond order in comparison to the neutral form, Figure 1c), thereby enabling cleavage and thus formation of sequence ions.

In other words, mobilization of ionizing protons to amide nitrogens has a facilitating effect, enabling amide bond cleavage which is of crucial importance in making peptide sequencing possible (in mass spectrometers operating under low-energy CID conditions). This hypothesis is strongly supported by energy-resolved surface-induced dissociation (SID)[6] and labeling experiments,[7a] quantum chemical calculations,[6c,7b,c] and recent spectroscopic[7f] and H/D exchange studies.[7d,e]

Detailed analysis of the available MS/MS, labeling, and theoretical data enabled the *mobile proton* model[6] of peptide fragmentation to be formulated. The mobile proton model states that protonated peptides with mobile protons (i.e., protons that can be easily transferred to various backbone amide sites) are expected to undergo facile dissociation and produce product ion spectra rich in sequence information. The model also states[6] that protonated peptides lacking mobile protons on the peptide backbone fragment less readily as more energy input is necessary to initiate fragmentation. Typical examples are those where the number of arginines equals or exceeds the number of ionizing protons[6e] or ions that contain only fixed charges.[8a] Doubly protonated peptides with two or more R residues (from missed cleavages during tryptic digestion or nontryptic digestion) and all MALDI-generated peptide ions with C-terminal R belong to this class. In some cases, proton sequestration by arginine can be strong enough that charge-remote fragmentation pathways become more active than their charge-directed counterparts, leading to selective fragmentation. For example, aspartic acid- and/or glutamic acid-containing peptides[6e,8−10] with sequestered ionizing protons often produce MS/MS spectra which are lacking in valuable sequence ions. This is thought to be due to the acidic residues enabling facile, selective cleavage of the amide bond on their C-terminal side, resulting in cyclic anhydride[6e,8,9] N-terminal fragments and normal C-terminal fragments. Despite this, detailed experimental studies[10,11] on peptide ions from MALDI have demonstrated that many such ions fragment well, even under the milder excitation generally applied in ion traps. Recent instrumental developments in ion-trapping technologies and peptide activation methods have enabled renewed interest in the use of MALDI ionization for peptide sequencing,[12] too. Furthermore, MALDI-generated peptide ions are routinely fragmented in time-of-flight/time-of-flight[11] (TOF/TOF) instruments, producing high-quality spectra for sequencing.

Prior studies elucidated some of the proton transfer pathways and amide bond-cleavage mechanisms of peptide ions with mobile protons.[5−7,13−15] In contrast, in the present paper we investigate the proton-driven amide bond-cleavage chemistry of peptides *lacking* mobile protons. The product ion spectra of singly protonated G_NR ($N = 2-4$) were acquired on MALDI-

(7) (a) Harrison, A. G.; Yalcin, T. *Int. J. Mass Spectrom.* **1997**, *165*, 339. (b) Csonka, I. P.; Paizs, B.; Lendvay, G.; Suhai, S. *Rapid Commun. Mass Spectrom.* **2000**, *14*, 417. (c) Paizs, B.; Csonka, I. P.; Lendvay, G.; Suhai, S. *Rapid Commun. Mass Spectrom.* **2001**, *15*, 637. (d) Jorgensen, T. J. D.; Gardsvoll, H.; Ploug, M.; Roepstorff, P. *J. Am. Chem. Soc.* **2005**, *127*, 2785. (e) Hermann, K. A.; Wysocki, V. H.; Vorpagel, E. R. *J. Am. Soc. Mass Spectrom.* **2005**, *16*, 1067. (f) Polfer, N. C.; Oomens, J.; Suhai, S.; Paizs, B. *J. Am. Chem. Soc.* **2007**, *129*, 5887.

(8) (a) Gu, C. G.; Tsaprailis, G.; Breci, L.; Wysocki, V. H. *Anal. Chem.* **2000**, *72*, 5804. (b) Tsaprailis, G.; Somogyi, A.; Nikolaev, E. N.; Wysocki, V. H. *Int. J. Mass Spectrom.* **2000**, *196*, 467–479.

(9) Yu, W.; Vath, J. E.; Huberty, M. C.; Martin, S. A. *Anal. Chem.* **1993**, *65*, 3015.

(10) Qin, J.; Chait, B. T. *Int. J. Mass Spectrom.* **1999**, *190/191*, 313.

(11) (a) Medzihradszky, K. F.; Campbell, J. M.; Baldwin, M. A.; Falick, A. M.; Juhasz, P.; Vestal, M. L.; Burlingame, A. L. *Anal. Chem.* **2000**, *72*, 552. (b) Falkner, J. A.; Kachman, M.; Veine, D. M.; Walker, A.; Strahler, J. R.; Andrews, P. C. *J. Am. Soc. Mass Spectrom.* **2007**, *18*, 850.

(12) (a) Strupat, K.; Kovtoun, V.; Bui, H.; Viner, R.; Stafford, G.; Horning, S. *J. Am. Soc. Mass Spectrom.* **2009**, *20*, 1451. (b) www.thermo.com/orbitrap.

(13) (a) Yalcin, T.; Khouw, C.; Csizmadia, I. G.; Peterson, M. R.; Harrison, A. G. *J. Am. Soc. Mass Spectrom.* **1995**, *6*, 1165. (b) Yalcin, T.; Csizmadia, I. G.; Peterson, M. B.; Harrison, A. G. *J. Am. Soc. Mass Spectrom.* **1996**, *7*, 233. (c) Nold, M. J.; Wesdemiotis, C.; Yalcin, T.; Harrison, A. G. *Int. J. Mass Spectrom. Ion Processes* **1997**, *164*, 137. (d) Polce, M. J.; Ren, D.; Wesdemiotis, C. *J. Mass Spectrom.* **2000**, *35*, 1391.

(14) (a) Paizs, B.; Lendvay, G.; Vékey, K.; Suhai, S. *Rapid Commun. Mass Spectrom.* **1999**, *13*, 525–533. (b) Rodriquez, C. F.; Cunje, A.; Shoeib, T.; Chu, I. K.; Hopkinson, A. C.; Siu, K. W. M. *J. Am. Chem. Soc.* **2001**, *123*, 3006–3012. (c) Paizs, B.; Suhai, S. *Rapid Commun. Mass Spectrom.* **2002**, *16*, 375–389. (d) Paizs, B.; Suhai, S. *J. Am. Soc. Mass Spectrom.* **2004**, *15*, 103–112.

(15) (a) Bythell, B. J.; Barofsky, D. F.; Pingitore, F.; Polce, M. J.; Wang, P.; Wesdemiotis, C.; Paizs, B. *J. Am. Soc. Mass Spectrom.* **2007**, *18*, 1291–1303. (b) Bythell, B. J.; Somogyi, A.; Paizs, B. *J. Am. Soc. Mass Spectrom.* **2009**, *20*, 618–624. (c) Bythell, B. J.; Erlekam, U.; Paizs, B.; Maitre, P. *Chem. Phys. Chem.* **2009**, *10*, 883–885.

TOF/TOF, ion trap, and FT-ICR mass spectrometers which are routinely used in large-scale proteomics studies. The observed fragmentation patterns indicate that these peptide ions fragment, producing *b* and *y* sequence ions despite no obviously mobile proton being available to facilitate amide bond cleavage. The mobilization pathways of all arginine side-chain, C-terminal carboxyl, and amidic protons along with the corresponding amide bond-cleavage pathways are considered in our detailed computational studies of the potential energy surface (PES). These data suggest that peptide ions lacking easily mobilizable protons do fragment on proton-driven pathways but that the basic amide bond-cleavage mechanisms and therefore the related dissociation chemistry are different from those active for ions with fully mobile protons.

2. Computations and Experiments

2.1. Computational Details. A recently developed conformational search engine[16] devised to deal with protonated peptides was used to scan the potential energy surfaces (PES) of protonated G_NR ($N = 2-4$). These calculations began with molecular dynamics simulations using the Insight II program (Biosym Technologies, San Diego, CA) in conjunction with the AMBER force field, modified in-house in order to enable the study of structures with oxygen- and nitrogen-protonated amide bonds, imine and oxazolone groups, and amide bond-cleavage transition structures (TS). During the dynamics calculations we used simulated annealing techniques to produce candidate structures for further refinement, applying full geometry optimization using the AMBER force field.[17] These optimized structures were analyzed by a conformer family search program developed in Heidelberg. This program groups optimized structures into families for which the most important characteristic torsion angles of the molecule are similar. The most stable species in the families were then fully optimized at the PM3, HF/3-21G, B3LYP/6-31G(d), and finally at the B3LYP/6-31+G(d,p) levels. Recent studies have shown that this model chemistry with an appropriate basis set provides good predictions of reaction barrier heights.[18] The conformer families were regenerated at each level, and only structurally nondegenerate conformers are recomputed at the next level to prevent wasting computer time (i.e., only one of *N* identical structures is recomputed at the next level). For the various protonation sites of $[G_2R + H]^+$ for example, 35000 structures were computed at the HF/3-21G//PM3 level, 4210 at the HF/3-21G level, 387 structures at the B3LYP/6-31G(d), and finally 298 structures at the B3LYP/6-31+G(d,p) level. For $[G_3R + H]^+$ and $[G_4R + H]^+$ we examined fewer possible protonation sites (only charge solvated and N-terminally protonated salt-bridge), but used more structures to characterize each conformer type (protonation site(s)) in keeping with the proliferation in system size. This ensured that the conformer calculations were truly representative of the protonation sites examined. All TSs were examined by vibrational analysis and then submitted to intrinsic reaction coordinate (IRC) calculations to determine which minima they connect. The total energies of the various structures are presented in Tables 1, 2, and 3 and in the Supporting Information (S1).

For the energetically most preferred structures we performed frequency calculations at the B3LYP/6-31G(d) level of theory. The relative energies were calculated by correcting the B3LYP/6-31+G(d,p) total energies for zero-point vibrational energy (ZPE) and/or thermal and entropy contributions determined from the unscaled B3LYP/6-31G(d) frequencies. The Gaussian set of programs[19] was used for all *ab initio* and DFT calculations.

Table 1. Total and Relative Energies, Free Energies, and Activation Entropies of the Various Minima and Transition Structures of $[GGR + H]^+$ Determined at the B3LYP/6-31+G(d,p) Level of Theory with the Relative Energies Corrected for Zero-Point Vibration Energy (ZPE) Using B3LYP/6-31G(d) Level of Theory[a]

structure	E_{Total} + ZPE /H	E_{rel}/ kcal mol^{-1}	ΔG_{298}/ kcal mol^{-1}	ΔS_{298}/ cal K^{-1} mol^{-1}
CS global minimum	–1022.732645	0.0	0.0	0.0
SB N-term. prot.	–1022.714126	11.6	13.5	–9.5
TS classical b_2-y_1	–1022.649274	52.3	52.9	–3.9
TS salt-bridge b_2-y_1	–1022.660782	45.1	47.7	–12.0
TS Imine enol b_2-y_1	–1022.655932	48.1	49.8	–8.7
TS anhydride b_2-y_1	**–1022.670941**	**38.7**	**41.0**	**–7.6**
TS to form the b_2-y_1 anhydride intermediate	–1022.681826	31.9	32.4	–3.6

[a] Bold-face type indicates the rate-determining step of the lowest energy b_n-y_m pathways.

Table 2. Total and Relative Energies, Free Energies, and Activation Entropies of the Various Minima and Transition Structures of $[GGGR + H]^+$ Determined at the B3LYP/6-31+G(d,p) Level of Theory with the Relative Energies Corrected for Zero-Point Vibration Energy (ZPE) Using B3LYP/6-31G(d) Level of Theory[a]

structure	E_{Total} + ZPE/H	E_{rel}/ kcal mol^{-1}	ΔG_{298}/ kcal mol^{-1}	ΔS_{298}/ cal K^{-1} mol^{-1}
CS global minimum	–1230.715796	0.0	0.0	0.0
SB N-term. prot.	–1230.694568	13.3	15.7	–10.7
TS salt-bridge b_2-y_2	**–1230.639572**	**47.8**	**50.6**	**–12.4**
TS imine enol b_2-y_2	–1230.627793	55.2	56.7	–7.5
TS anhydride b_2-y_2	–1230.648463	42.3	42.3	–0.1
TS to form the b_2-y_2 anhydride intermediate	–1230.636070	50.0	50.7	–4.1
TS salt-bridge b_3-y_1	–1230.636927	49.5	52.7	–14.2
TS Imine enol b_3-y_1	–1230.640428	47.3	49.2	–8.8
TS anhydride b_3-y_1	**–1230.650115**	**41.2**	**41.1**	**–1.2**
TS to form the b_3-y_1 anhydride intermediate	–1230.656188	37.4	39.9	–11.6

[a] Bold-face type indicates the rate-determining step of the lowest energy b_n-y_m pathways.

Table 3. Total and Relative Energies, Free Energies, and Activation Entropies of the Various Minima and Transition Structures of $[GGGGR + H]^+$ Determined at the B3LYP/6-31+G(d,p) Level of Theory with the Relative Energies Corrected for Zero-Point Vibration Energy (ZPE) Using B3LYP/6-31G(d) Level of Theory[a]

structure	E_{Total} + ZPE/H	E_{rel}/ kcal mol^{-1}	ΔG_{298}/ kcal mol^{-1}	ΔS_{298}/ cal K^{-1} mol^{-1}
CS global minimum	–1438.693998	0.0	0.0	0.0
SB N-term. prot.	–1438.682147	7.4	11.2	–16.4
TS salt-bridge b_2-y_3	–1438.614512	49.9	53.8	–17.1
TS imine enol b_2-y_3	–1438.612790	51.0	53.6	–12.3
TS anhydride b_2-y_3	**–1438.620020**	**46.4**	**50.7**	**–18.6**
TS to form the b_2-y_3 anhydride intermediate	–1438.620827	45.9	50.5	–14.9
TS salt-bridge b_3-y_2	**–1438.622604**	**44.8**	**47.8**	**–13.3**
TS imine enol b_3-y_2	–1438.610865	52.2	55.2	–13.5
TS anhydride b_3-y_2	–1438.617579	48.0	53.1	–21.9
TS to form the b_3-y_2 anhydride intermediate	–1438.611557	51.7	55.9	–21.2
TS Salt-bridge b_4-y_1	–1438.616297	48.8	50.0	–14.9
TS imine enol b_4-y_1	–1438.612846	50.9	55.7	–20.9
TS anhydride b_4-y_1	**–1438.625916**	**42.7**	**45.7**	**–13.5**
TS to form the b_4-y_1 anhydride intermediate	–1438.639148	34.4	38.3	–17.5

[a] Bold-face type indicates the rate-determining step of the lowest energy b_n-y_m pathways.

(16) (a) Wyttenbach, T.; Paizs, B.; Barran, P.; Breci, L.; Liu, D.; Suhai, S.; Wysocki, V. H.; Bowers, M. T. *J. Am. Chem. Soc.* **2003**, *125*, 13768. (b) Bleiholder, C.; Osburn, S.; Williams, T. D.; Suhai, S.; Van Stipdonk, M.; Harrison, A. G.; Paizs, B. *J. Am. Chem. Soc.* **2008**, *130*, 17774.

(17) Case, D. A.; et al. *AMBER 99*; University of California: San Francisco, 1999.

(18) (a) Heaton, A. L.; Armentrout, P. B. *J. Am. Chem. Soc.* **2008**, *130*, 10227. (b) El Aribi, H.; Orlova, G.; Rodriquez, C. F.; Almeida, D. R. P.; Hopkinson, A. C.; Siu, K. W. M. *J. Phys. Chem. B* **2004**, *108*, 18743.

2.2. Mass Spectrometry. G_2R, G_3R, and G_4R were synthesized using standard solid-phase protocols the details of which can be found in ref 20.

MALDI-TOF/TOF tandem mass spectrometry experiments were performed on a Burker Ultraflex III instrument (Billerica, MA). The matrix was prepared by dissolving α-cyano-4-hydroxycinnamic acid in acetonitrile/water/trifluoroacetic acid/monoammonium phosphate (6 mg/mL) 47/47/0.1/6 (vol:vol) solution at a concentration of 2 mg/mL. The G_NR peptides were dissolved in acetonitrile/water/trifluoroacetic acid 50/50/0.1 (vol:vol) solution at a concentration of 100 μg/mL. The sample solutions were then prepared by mixing the matrix/peptide solutions. 100 fmol of peptide was placed on each spot. The "LIFT" aquisition mode was applied with standard conditions for the TOF/TOF experiments.

MS and low energy (eV) CID (He) MS/MS experiments were carried out in a Thermoelectron (Finnigan) (San Jose, CA) LCQ Classic ion trap (IT) instrument using electrospray ionization (ESI) to form the singly charged $[M + H]^+$ precursor ion. Peptides were dissolved in CH_3OH/H_2O = 1:1 containing 2% acetic acid in a concentration range of 50−80 μmol and were sprayed with conventional ESI conditions (e.g., 4.5 kV needle voltage, 200 V capillary entrance voltage, 60 sheathgas flow (in arbitrary units), 200 °C capillary temperature, and 5 μL/min flow rate). Helium was used as the collision gas with a conventional pressure (a few times 10^{-5} Torr) in the ion trap. Relative collision energies were 25% with a q value of 0.250.

A Bruker 9.4 T FT-ICR instrument was also used for CID experiments. Here CID with Ar as the collision gas was used as the ion activation technique to induce fragmentation of the singly protonated precursor ions. Singly protonated peptides were generated from ca. 10 μM acetonitrile/H_2O 1:1 solutions (containing 0.1% formic acid) by the electrospray source.

3. Results and Discussion

3.1. CID of Protonated G_NR (N = 2−4). The MALDI-TOF/TOF, IT, and FT-ICR MS/MS spectra of $[G_NR + H]^+$ (N = 2−4) are summarized in Tables S2−S4 (SI). These experiments yielded similar peaks but with differences in fragment ion abundance and the degree of small neutral losses. All spectra contain the sequence informative y_m peaks with significant abundances along with peaks resulting from small neutral losses (predominantly ammonia). Additionally, further sequence informative b_n ions are present in most spectra. In general the C-terminal y peaks are more abundant than the N-terminal b peaks. For example, cleavage of the G−R amide bond of $[G_2R + H]^+$ can lead to b_2 and y_1 ions; in the FT-ICR only the latter is observed, while in the IT and TOF/TOF both peaks are present, but y_1 is much more abundant. In all three cases, the peaks from the b_{X-1}-y_1 pathway (where X is the total number of residues; $X = n + m$) arising from cleavage of the G−R amide bonds are more abundant than those produced by cleavages of other amide bonds. For example, for G_4R fragments from cleavage of the G(2)−G(3) amide bond ($b_2 + y_3$) are less abundant than fragments arising from cleavages of G(3)−G(4) ($b_3 + y_2$) and G(4)−R ($b_4 + y_1$). Consideration of the satellite ions complicates this picture somewhat, but the general trend holds. As the N-terminal fragments get larger (i.e., b_2:b_3:b_4) generally their relative abundance also increases in keeping with the enlarged proton affinity.

3.2. Structures of Protonated G_NR (N = 2−4). The $[M + H]^+$ ions of G_NR can in principle have two major types of protonation, namely charge-solvation (CS) and salt-bridge (SB) stabilized structures. Both classes of $[M + H]^+$ ions contain a protonated Arg side chain. In a CS structure the two termini are neutral (for G_2R see Figure 2a), whereas in a SB structure the C-terminus is deprotonated, and another backbone site is protonated (for G_2R see Figure 2c). The relative stability of the CS and SB forms depends strongly on the sequence and size of the peptide. Our calculations indicate that the energetically most favored structures of protonated G_NR (N = 2−4) feature CS structures with the guanidinium group solvated by backbone carbonyl oxygens. The lowest energy salt-bridge structures where the formal C-terminal acidic proton is transferred to the N-terminus are less favored. However, the gap between the CS and N-terminally protonated SB forms is relatively small for the protonated G_NR series studied (7.4−13.3 kcal mol^{-1}, Tables 1−3).

More efficient stabilization of the SB charge centers via increased H-bonding with electron-donating groups is expected to occur in larger systems.[21−24] For example, BIRD experiments[22] and calculations[23] indicate that singly protonated bradykinin forms a SB in the gas phase. On the other hand, ion mobility measurements[24] were unable to distinguish between the two forms due to the significant structural similarity between some of the SB and CS structures (corresponding to the measured cross-section). It is conceivable that the ease of fragmentation found for some larger protonated peptides lacking easily moblizable protons is partially due to the most stable structures being salt-bridges. If this were the case, then the initial energy needed to mobilize a proton away from the C-terminus or guanidinium group would in effect already be provided by the SB global minimum. Subsequent proton transfers to the amide nitrogens would of course still be necessary to enable amide bond cleavage.

3.3. Mobilization of an Arginine Side Chain Sequestered Proton and Cleavage of the G−R Amide Bond on the Classical b_2-y_1 Pathway for $[G_2R + H]^+$. The classical[4,6,13−15] b_n-y_m pathway (illustrated in Scheme 1 for G_2R) is a multistep process that is initiated by proton transfer from the charged guanidinium moiety. Our calculations indicate that the corresponding proton transfer pathways require substantial energy due to the high basicity of the guanidino group. These proton transfers result in structures that feature the neutral Arg side chain and protonation at a backbone site (Figure 2b). The energetically most favored such structure involves protonation at the G−R amide oxygen (relative energy at 16.9 kcal mol^{-1}). Subsequent proton transfer to the N-terminal amide O or the N-terminal amino group is more energetically demanding. Populating the amide nitrogen sites critical for amide bond cleavage requires at least 40 kcal mol^{-1} relative energy. This is significantly more energy than is necessary to fragment singly protonated peptides lacking a basic residue (∼30 kcal mol^{-1}).[4,13−15]

These amide nitrogen protonated structures were found to be intermediates on the classical[4,6,13−15] oxazolone b_n-y_m pathways for systems with easily mobilizable protons. In contrast, our calculations indicate that for $[GGR + H]^+$, the proton transfer to the (G2)−(R) amide nitrogen protonation site and the subsequent amide bond cleavage occur in a complicated,

(19) Frisch, M. J.; et al. *Gaussian 03*; Gaussian Inc.: Pittsburgh, PA, 2003.
(20) Paizs, B.; Suhai, S.; Hargittai, B.; Hruby, V. J.; Somogyi, A. *Int. J. Mass Spectrom.* **2002**, *219*, 203.
(21) Wyttenbach, T.; Bushnell, J. E.; Bowers, M. T. *J. Am. Chem. Soc.* **1998**, *120*, 5098.
(22) Schnier, P. D.; Price, W. D.; Jockusch, R. A.; Williams, E. R. *J. Am. Chem. Soc.* **1996**, *118*, 7178–7189.
(23) Rodriquez, C. F.; Orlova, G.; Guo, Y.; Li, X.; Siu, C.-K.; Hopkinson, A. C.; Siu, K. W.; M, *J. Phys. Chem. B.* **2006**, *110*, 7528–7537.
(24) Wyttenbach, T.; von Helden, G.; Bowers, M. T. *J. Am. Chem. Soc.* **1996**, *118*, 8355–8364.

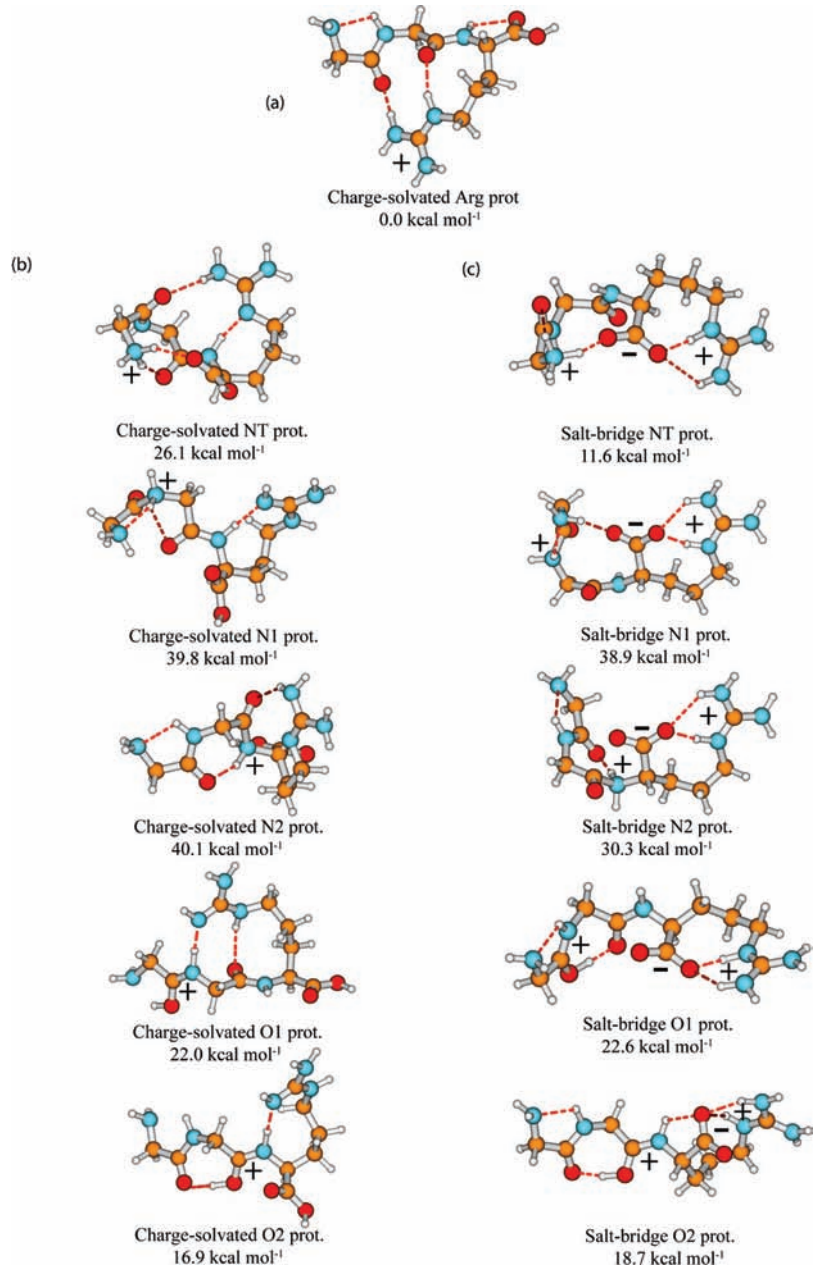

Figure 2. Structures and relative energies of some of the minima of $[GGR + H]^+$ (B3LYP/6-31+G(d,p) energies corrected for B3LYP/6-31G(d) zero-point vibration energy). The sites of charges (approximate) are indicated by ± signs. (a) The global minimum CS structure; (b) charge-solvated structures generated by mobilization of one of the guanidium protons; (c) salt-bridge structures generated by mobilization of the C-terminal carboxyl proton (the nonarginyl protonation site is listed).

concerted process; i.e. the protonated guanidine group transfers a proton to the amide nitrogen, and this is immediately followed by nucleophilic attack of the (G1) carbonyl oxygen to the (G2) carbonyl carbon, eliciting amide bond cleavage. This mechanism involves a transition structure (Figure 3) that requires 52.3 kcal mol^{-1} relative energy to access. Following the dissociation a short-lived proton-bound dimer of R and 2-amino-methyl-5-oxazolone is formed which can undergo numerous proton transfers between the monomers.[14] As R is more basic than 2-aminomethyl-5-oxazolone,[25] the y_1 peak (protonated R) should be preferentially formed rather than the b_2 ion which is consistent with the spectra (Tables S2−S4, SI).

The classical[4,6,13−15] oxazolone b_n-y_m barrier for protonated G_2R is ∼1.8 times that of the equivalent reaction for $[GGG + H]^+$, which has a barrier of ∼30 kcal mol^{-1} (Table S5, SI). This result supports the analytical finding[6,10,26] that singly charged peptides containing arginine require more energy to fragment than do those lacking basic residues or with an additional ionizing proton. However, this 52.3 kcal mol^{-1} barrier is significantly higher than those found previously by Schnier et al.[22] for formation of sequence ions for structurally similar model peptides. Schnier et al.[22] demonstrated with blackbody infrared radiative dissociation data on variants of singly protonated bradykinin, that both the activation energy and the most facile reaction(s) are strongly affected by the chemical makeup

(25) (a) Rodriquez, C. F.; Shoeib, T.; Chu, I. K.; Siu, K. W. M.; Hopkinson, A. C. *J. Phys. Chem. A* **2000**, *104*, 5335–5342. (b) Bleiholder, C.; Suhai, S.; Paizs, B. *J. Am. Soc. Mass Spectrom.* **2006**, *17*, 1275–1281.
(26) Wee, S.; O'Hair, R. A. J.; McFadyen, W. D. *Int. J. Mass Spectrom.* **2004**, *234*, 101.

Scheme 1. Mobilization of an R Side-Chain Proton Followed by Cleavage of the (G2)−(R) Amide Bond of $[G_2R + H]^+$ on the Classical Oxazolone b_n-y_m Pathway

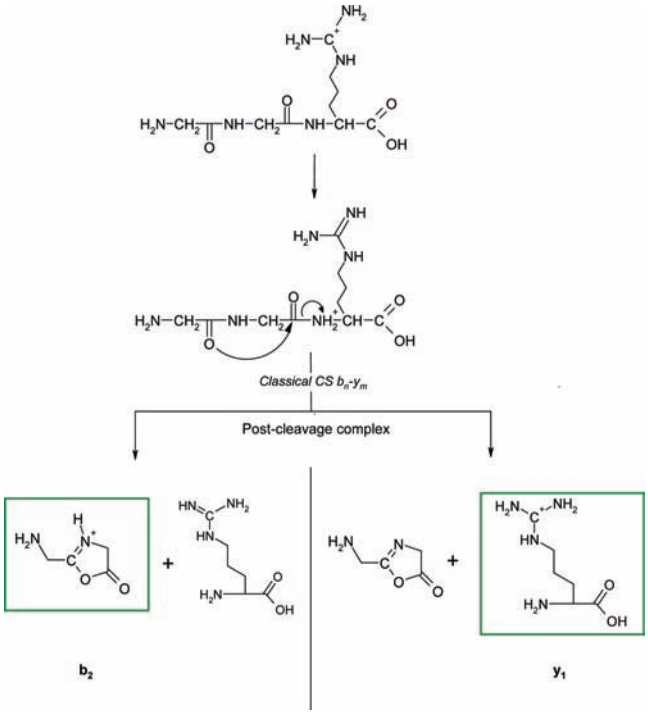

of the system under study. Their data demonstrate that for these comparatively large systems, threshold energies in the range of ~20−35 kcal mol^{-1} are possible. Laskin et al.[27] have also found that the composition of the peptide can strongly affect the calculated dissociation barriers. These authors found that the presence of basic residues, particularly arginine, led to increased dissociation barriers up to ~40 kcal mol^{-1} for large systems and argued for the importance of the negative activation entropies associated with peptide fragmentation barriers.[27] Additionally, Schnier et al.'s data show[22] that many of the least energetically demanding dissociation pathways for these peptides do not produce *b* and/or *y* ions, indicating that these barriers must require additional energy to overcome. In line with these findings our calculations indicate that other nonclassical b_n-y_m mechanisms should be active, producing the sequence ions observed in our spectra. We will show that these new mechanisms employ differing means of proton mobilization (with associated TSs) and are much less energetically demanding than the classical b_n-y_m mechanism discussed in the preceding text.

3.4. Mobilization of the C-Terminal Carboxyl Proton: Formation of Salt-Bridge Intermediates for Protonated G_2R. The first alternative means of proton mobilization involves utilization of the C-terminal carboxylic acid proton. Transfer of this proton leads to salt-bridge (SB) intermediates that feature a negatively charged C-terminus, a positively charged R side chain, and an additional backbone site of protonation. The gap between the most stable charge-solvated (CS) and N-terminally protonated SB structure is relatively small for protonated G_2R (11.6 kcal mol^{-1}, Table 1). To assess the feasibility of interconversion between the charge-solvated and salt-bridge forms we performed detailed scans of the possible proton

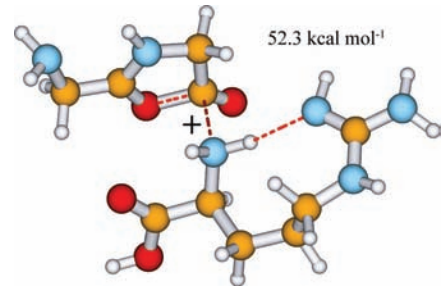

Figure 3. Structure of the classical b_2-y_1 TS of $[GGR + H]^+$ determined at the B3LYP/6-31+G(d,p) level of theory. The relative energy is included for clarity.

transfer pathways. These calculations indicate that the electronic energy of the most favored CS → SB transition structure (Figure S1, SI) is only 1.6 kcal mol^{-1} higher than the corresponding SB structure. This small barrier is completely eliminated after correction for ZPE, indicating a very facile CS → SB transition if the necessary internal energy is available. Therefore, the CS → SB transition is not kinetically controlled. This is in keeping with the proposals of Leffler and Hammond.[28]

After the initial CS → SB transition the formerly carboxylic proton can transfer to other amide O and N protonation sites. While the amide O protonated SB structures (Figure 2c) are energetically slightly less favored than the corresponding CS structures formed by mobilization of one of the guanidium protons (Figure 2b), the opposite is true for the amide N protonated species. Population of the SB (G2)−(R) amide nitrogen protonated structure (Figure 2c) requires 30.3 kcal mol^{-1} relative energy, while the analogous CS structure is at 40.1 kcal mol^{-1} relative energy (Figure 2b). This indicates that amide N protonated structures that are critical for initiating amide bond cleavage are more easily accessed via salt-bridge structures than for the charge-solvated forms of protonated G_2R.

3.5. Rearrangement Reactions and Dissociation of Salt-Bridge Structures: the Salt-Bridge b_n-y_m and Anhydride b_n-y_m Pathways for $[G_2R + H]^+$. Two possible reactive fates of the SB structures of $[G_2R + H]^+$ with the formerly carboxylic proton residing at the (G2)−(R) amide nitrogen (30.3 kcal mol^{-1} relative energy) are shown in Scheme 2. In Reaction I, nucleophilic attack of the N-terminal amide oxygen on the (G2) carbonyl carbon of the protonated amide bond leads to a SB stabilized b_n-y_m-type amide bond cleavage (TS 45.1 kcal mol^{-1}, Figure 4a, Scheme 2). This is over 7 kcal mol^{-1} more energetically favorable than the TS obtained via mobilization of an arginine side-chain proton (52.3 kcal mol^{-1}, Scheme 1). The SB stabilized dimer of zwitterionic R and protonated 2-aminomethyl-5-oxazolone formed after crossing this TS can then undergo numerous proton transfers and dissociate to form either y_1 or b_2 ions.

Alternatively in Reaction II, nucleophilic attack of a carboxylate oxygen on the (G2) carbonyl carbon of the protonated amide bond (Reaction II_a, Scheme 2) can lead to formation of an anhydride intermediate (TS at 31.9 kcal mol^{-1}, relative energy, Figure 4b). Attack on the N-terminal carbonyl of the −C(O)−O−C(O)− anhydride group, by the (G1) carbonyl oxygen then cleaves the C(O)−O bond, generating a salt-bridge dimer of zwitterionic arginine and protonated 2-aminomethyl-5-oxazolone. This reaction has the lowest threshold energy at 38.7 kcal mol^{-1} (Figure 4c, Table 1) of the pathways explored

(27) (a) Laskin, J.; Bailey, T. H.; Futrell, J. H. *Int. J. Mass Spectrom.* **2002**, *222*, 312. (b) Laskin, J.; Bailey, T. H.; Futrell, J. H. *Int. J. Mass Spectrom.* **2004**, *234*, 89–99. (c) Lioe, H.; Laskin, J.; Reid, G. E.; O'Hair, R. A. J. *J. Phys. Chem. A* **2007**, *111*, 10580.

(28) (a) Leffler, J. E. *Science* **1952**, *117*, 340–341. (b) Hammond, G. S. *J. Am. Chem. Soc.* **1955**, *77*, 334–338.

Scheme 2. Mobilization of the C-Terminal Carboxylic Acid Proton Followed by Cleavage of the (G2)−(R) Amide Bond of $[G_2R + H]^+$ [a]

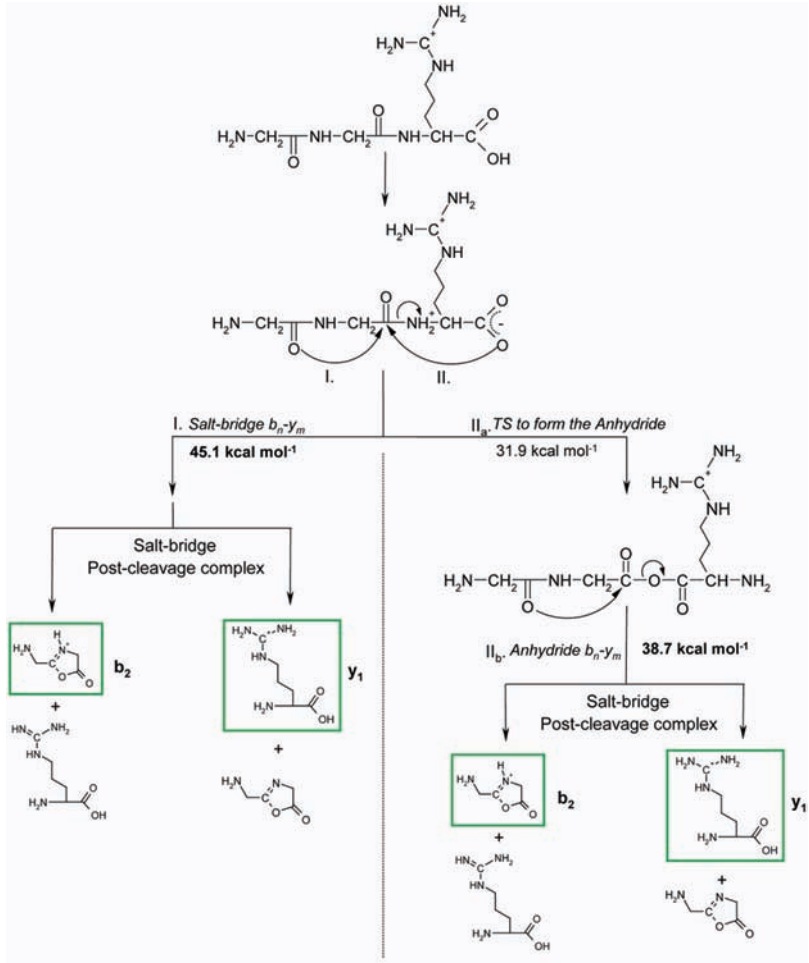

[a] Reaction I involves formation of b_2 and y_1 ions through a salt-bridge stabilized b_n-y_m transition structure. Reaction II involves anhydride formation then cleavage of the CO−O bond in the b_n-y_m transition structure. Relative energies are included for clarity. Bold-face type indicates the highest barrier in each mechanism.

for $[G_2R + H]^+$. The resulting SB dimer forms b_2 or y_1 ions as described in the preceding. It should be noted that an analogous anhydride intermediate was proposed by Farrugia et al.[29] to explain the very similar MS/MS spectra of protonated GR and RG, although the proposed mechanisms of formation are quite different. Farrugia et al.[29] suggested forming this anhydride from an oxazolone alcohol via a four-center proton transfer, with concerted amide bond cleavage. This oxazolone alcohol is a stable species and so was a potential intermediate. However, this requires an energetically unfavorable[7b,c] (>50 kcal mol^{-1}) four-center proton transfer reaction which would be rate-limiting for this mechanism. Our mechanism utilizes protonation of the (G2)−(R) amide nitrogen in a salt-bridge and is a much less energetically demanding means of forming the anhydride.

3.6. Imine Enol b_n-y_m Pathways Involving Amidic Proton Mobilization. Another proton mobilization pathway that has received little or no attention in the past involves amidic protons. This mobilization pathway converts the −CO−NH− amide bonds into imine enol structures (−COH=N−, Figure 5a). The relative energies of these structures are surprisingly low at 11.3 and 11.8 kcal mol^{-1} respectively for the G(1)−G(2) and G(2)−R imine enol forms. There exist several ways of forming these structures, the exhaustive details of which will be published elsewhere for a system where this method of proton mobilization is necessary to enable sequence ion formation. Briefly, one of the possible pathways initially involves protonation at the appropriate amide oxygen (−COH$^+$−NH− moiety). This significantly increases the acidity of the amidic proton thereby facilitating the subsequent transfer of this proton to another protonation site.

During our systematic scans of the potential energy surface of protonated G_2R we found that such imine enol structures can, in principle, undergo reactions that lead to cleavage (Scheme 3, Figure 5b) of the amide bond C-terminal to the imine enol moiety. The proton transfer and bond-cleavage reactions occur in a complex concerted process. Transfer of the hydroxyl proton to the (G2)−(R) amide nitrogen is followed by nucleophilic attack of the G(1) carbonyl O on the G(2) carbonyl carbon cleaving the (G2)−(R) amide bond (Scheme 3, threshold energy at 48.1 kcal mol^{-1}). After amide bond cleavage a proton-bound dimer of protonated arginine and 2-aminomethyl-5-oxazolone is formed. Proton transfers within the dimer can occur prior to dissociation to form y_1 or b_2 ions as described previously. While not as energetically favorable as the SB and anhydride b_n-y_m pathways (Scheme 2), this class of fragmentation pathway is more favorable than the classical b_n-y_m pathway (Scheme 1)

(29) Farrugia, J. M.; O'Hair, R. A. J. *Int. J. Mass Spectrom.* **2003**, *222*, 229–242.

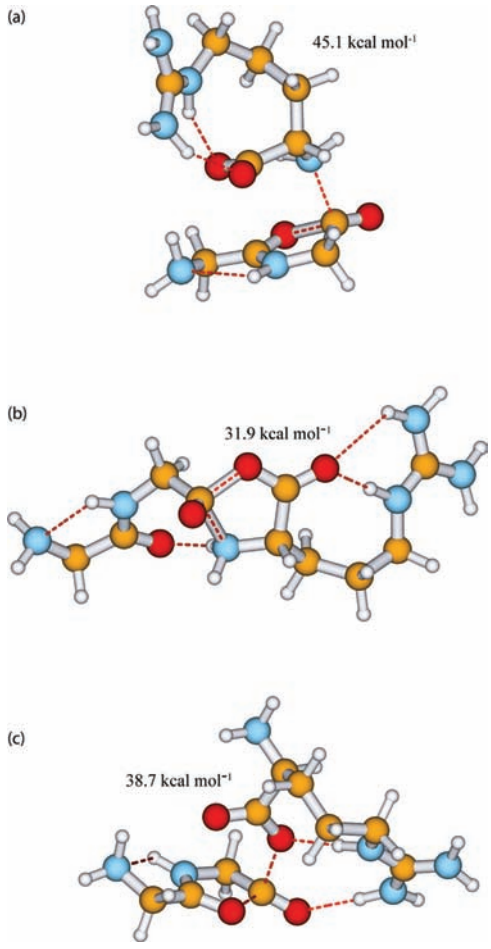

Figure 4. Structure and relative energy of the (a) salt-bridge b_2-y_1 TS, (b) the TS to form the b_2-y_1 anhydride intermediate and the (c) anhydride b_2-y_1 TS of $[GGR + H]^+$ determined at the B3LYP/6-31+G(d,p) level of theory with the relative energies corrected for zero-point vibration energy (ZPE) using B3LYP/6-31G(d) level of theory.

for protonated G_2R. Consequently, this mechanism is likely to be active for systems that feature an amidated or an esterified C-terminus[30] where the SB amide bond-cleavage pathways cannot occur. Furthermore, it is likely that peptide ions that only have fixed charges[8] fragment on this pathway too.

3.7. Rearrangement Reactions and Dissociation Pathways of $[G_3R + H]^+$ and $[G_4R + H]^+$: How General Are the New Mechanisms? To test if these mechanisms were relevant in larger peptides, the threshold energetics of the amide bond cleavages on the SB b_n-y_m, anhydride b_n-y_m, and imine enol b_n-y_m, pathways were calculated for protonated G_3R and G_4R. The corresponding data are presented in Tables 2 and 3. A comparison of the threshold energies of all three systems are presented in Figure 6. Additionally, Figures S2 and S3 (SI) show the most favorable b_n-y_m transition structures for the protonated G_3R and G_4R, respectively.

In order for the mechanisms involving anhydride bond cleavage to be active, the anhydride species must obviously be formed first (Reaction II_a, Scheme 2). Consequently, both reactions II_a and II_b must be considered when evaluating the applicability of this pathway (Scheme 2). For cleavage of the C-terminal amide bond the anhydride b_{X-1}-y_1 mechanism (X is the number of amino acid residues in the peptide) was the most energetically favorable in each of the systems we studied. For all these cases formation of the anhydride is energetically less

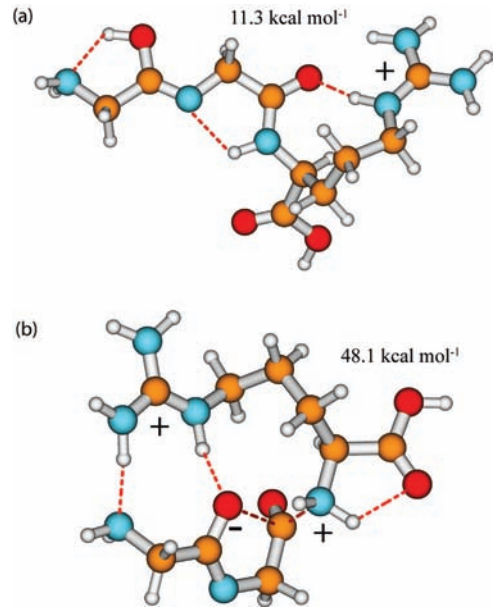

Figure 5. Structure and relative energies of the (a) G(1)−G(2) imine enol and the (b) imine enol b_2-y_1 TS of $[GGR + H]^+$ determined at the B3LYP/6-31+G(d,p) level of theory with the relative energies corrected for zero-point vibration energy (ZPE) using B3LYP/6-31G(d) level of theory.

Scheme 3. Mobilization of an Amidic Proton Followed by Cleavage of the (G2)−(R) Amide Bond of $[G_2R + H]^+$

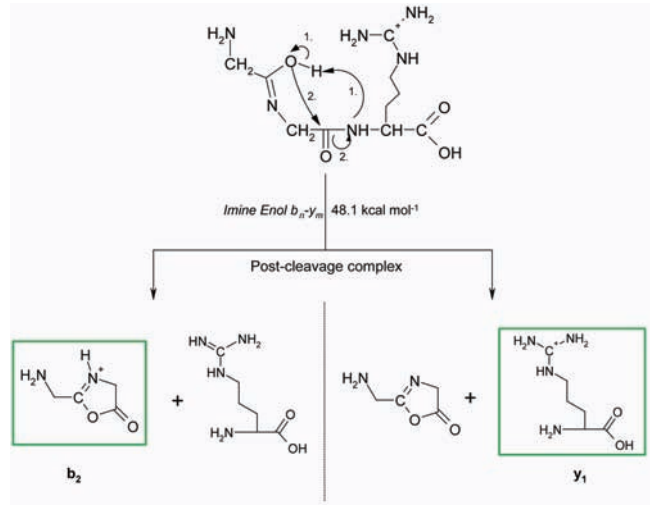

demanding than subsequent cleavage of the CO−O bond; thus, the second reaction is likely to be rate limiting. The SB b_{X-1}-y_1 and imine enol b_{X-1}-y_1 pathways both have significantly higher threshold energies so these are likely to be less active in the cleavage of the C-terminal amide bond of $[G_NR + H]^+$.

In the next step we examined whether the anhydride b_n-y_m mechanism is generally active or limited to the C-terminal amide bond. For amide bonds located far from the C-terminus this reaction is likely to be accompanied by large negative entropy changes. However, our calculations on $[G_4R + H]^+$ indicate that the anhydride b_n-y_m pathway is the energetically most favored mechanism for cleavage of the G(2)−G(3) amide bond with threshold energy at 46.4 kcal mol^{-1} and that the entropic component is similar to the salt-bridge and imine enol mechanisms (Table 3). An 11-membered ring transition structure is formed to cleave the amide bond and produces the new anhydride conformer relocating the previously C-terminal

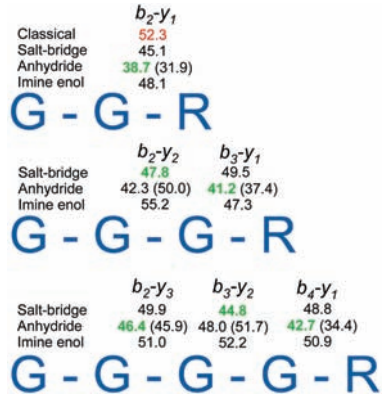

Figure 6. Summary of the b_n-y_m rate-limiting TSs for $[G_NR + H]^+$ ($N = 2-4$). Relative energies are in kcal mol^{-1}. The lowest calculated threshold energy for each pathway is highlighted in green. The classical b_2-y_1 calculated threshold energy is highlighted in red.

Scheme 4. Formation of the Anhydride Intermediate on the Anhydride b_2-y_3 Pathway[a]

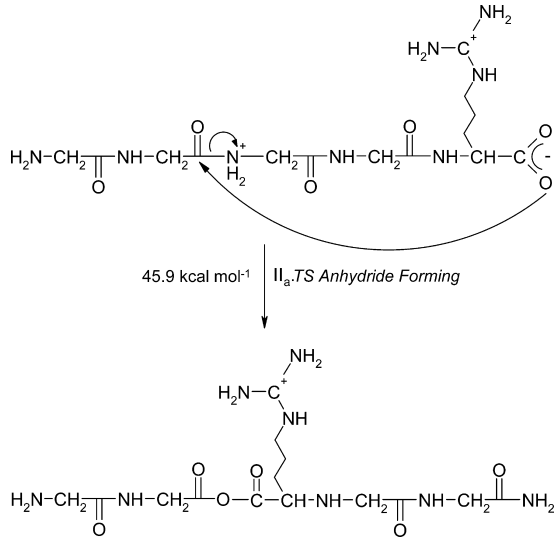

[a] Relative energies are included for clarity.

arginine R(5) at the nominally third position 'facing' the opposite direction (i.e., G(1)G(2)-o-(5)R(4)G(3)G, Scheme 4). Consequently, the related chemistry is not limited to the cleavage of the C-terminal amide bond. From the anhydride intermediate b_2 and y_3 ions can be formed by cleaving the anhydride linkage and forming a salt-bridge dimer of 2-aminomethyl-5-oxazolone and zwitterionic GGR.

It is worth noting here that fragmentation of the rearranged anhydride structure at amide bonds C-terminal to the anhydride moiety can in principle lead to formation of *nondirect* sequence ions via the loss of formerly internal residues.[16b,31] Additionally, it is conceivable that aspartic and glutamic acid residues could also produce this type of anhydride-forming reaction. Some support for this posibility comes from the selective fragmentation observed on the C-terminal side of acidic residues, where cyclic anhydride-terminated *b* ions[9] have been proposed and supported by tandem MS[6e,8] and H/D[7e] exchange studies. Our laboratory is currently studying the related fragmentation phenomena to see if this new scenario is a general occurrence in tandem mass spectra of protonated peptides.

The anhydride b_{X-2}-y_2 pathway is less favorable than the salt-bridge b_{X-2}-y_2 pathway for $[G_3R + H]^+$ and $[G_4R + H]^+$ (Tables 2 and 3). This is because formation of the anhydride intermediate necessitates a strained, eight-membered ring transition structure which is less energetically favorable than the corresponding SB b_{X-2}-y_2 transition structure. The imine enol mechanism is generally less energetically favorable than the anhydride b_n-y_m or SB b_n-y_m pathways. Overall, the combination of the various pathways enables a qualitative rationalization of the experimentally observed amide bond-cleavage tendencies (section 3.1), a situation not possible with any of the individual pathways on their own. For example, fragments from the G(2)−G(3) amide bond ($b_2 + y_3$) are less abundant than fragments arising from cleavages of G(3)−G(4) ($b_3 + y_2$) and G(4)−R ($b_4 + y_1$) for protonated G_4R. This tendency is explained by the calculated threshold energies at 46.4, 44.8, and 42.7 kcal mol^{-1} for the anhydride b_2-y_3, SB b_3-y_2, and anhydride b_4-y_1 pathways, respectively. Additionally, for $[G_3R + H]^+$ the peaks resulting from the anhydride b_3-y_1 pathway are considerably more abundant than those from the SB b_2-y_2 pathway. This follows from the 6.6 kcal mol^{-1} difference in threshold energies.

Similarly to the calculations of Laskin et al.[27] we found negative activation entropies for the amide bond-cleavage pathways. This is probably due to the reduction in conformational space accessible by salt-bridge structures in general, along with the need for good solvation of the charge centers in the transition structures. This necessarily limits the likelihood of 'open' structures similar to the charge solvated global minima being the most energetically favorable b_n-y_m transition structures. This is also in keeping with earlier predictions for salt-bridge versus charge-solvated structures.[21,22]

Conclusions

Our computed amide bond-cleavage threshold (TS) energies for protonated G_NR support the experimental finding that the fragmentation chemistry of protonated peptides lacking easily mobilizable protons differs from that of those featuring an easily mobilizable proton. For these systems, the C-terminal carboxylic acid proton is mobilized enabling fragmentation on pathways with salt-bridge intermediates, either with or without anhydride formation. Alternatively, mobilization of amidic protons leads to structures with the −COH=N− moiety from which cleavage of the C-terminally next amide bond can occur. The combination of these chemistries offers an explanation for the formation of *b* and *y* ions from MALDI-generated tryptic peptides (terminated with R) and fragmentation of peptide ions where the number of highly basic R residues is equal to or exceeds the number of mobile protons.

Acknowledgment. B.J.B. thanks the DKFZ for a guest scientist fellowship. B.P. and S.S. are grateful for financial support from the Landesstiftung Baden-Württemberg (P-CS-Prot/57). B.P. thanks the Deutsche Forschungsgemeinschaft for a Heisenberg fellowship.

Supporting Information Available: Structures and total energies of the species presented in the text, CID spectra of protonated G_NR, and complete references 17 and 19. This material is available free of charge via the Internet at http://pubs.acs.org.

JA903883Z

(30) Mouls, L.; Subra, G.; Aubagnac, J.-L.; Martinez, J.; Enjalbal, C. *J. Mass Spectrom.* **2006**, *41*, 1470–1483.
(31) Harrison, A. G.; Young, A. B.; Bleiholder, C.; Suhai, S.; Paizs, B. *J. Am. Chem. Soc.* **2006**, *128*, 10364.